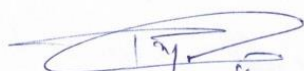


CERTIFICATE

It is certified that the work contained in the thesis entitled "*Natural and Synthetic based Polymeric Nanoparticles for Drug Delivery*" by "*Rahul Kumar*" has been carried out under my supervision and that this work has not been submitted elsewhere for a degree. It is further certified that the student has fulfilled all the requirements of Comprehensive, Candidacy and SOTA.



Dr. Pranjal Chandra
(Supervisor)
School of Biochemical Engineering
Indian Institute of Technology
(Banaras Hindu University),
Varanasi-221005
Assistant Professor
School of Biochemical Engineering
Indian Institute of Technology (BHU)
Varanasi-221005, U.P., INDIA



Prof. Vikash Kumar Dubey
(Co-supervisor)
School of Biochemical Engineering
Indian Institute of Technology
(Banaras Hindu University),
Varanasi-221005

डॉ० विकास कुमार दुबे
Dr. Vikash Kumar Dubey
आचार्य
Professor
जीव रासायनिक अभियांत्रिकी स्कूल
School of Biochemical Engineering
भारतीय प्रौद्योगिकी संस्थान
Indian Institute of Technology
(बनारस हिंदू विश्वविद्यालय) वाराणसी-221005
(B.H.U.) Varanasi-221005

DECLARATION BY THE CANDIDATE

I, **Rahul Kumar**, certify that the work embodied in this thesis is my own bona fide work and carried out by me under the supervision of **Dr. Pranjal Chandra** from “**July, 2016 to June, 2022**”, at the School of Biochemical Engineering, Indian Institute of Technology (Banaras Hindu University), Varanasi. The matter embodied in this thesis has not been submitted for the award of any other degree/diploma.

I declare that I have faithfully acknowledged and given credits to the research workers wherever their works have been cited in my work in this thesis. I further declare that I have not willfully copied any other's work, paragraphs, text, data, results, *etc.*, reported in journals, books, magazines, reports dissertations, theses, *etc.*, or available at websites and have not included them in this thesis and have not cited as my own work.

Date: 30/06/2022

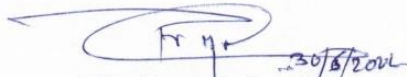
Place: Varanasi

Rahul Kumar
Signature of the Student

(Rahul Kumar)

CERTIFICATE BY THE SUPERVISOR

It is certified that the above statement made by the student is correct to the best of our knowledge.



(Dr. Pranjal Chandra)

Supervisor

Assistant Professor

School of Biochemical Engineering

Indian Institute of Technology

(Banaras Hindu University)

Varanasi - 221005

Dr. Pranjal Chandra Ph.D.
Assistant Professor
School of Biochemical Engineering
Indian Institute of Technology (BHU)
Varanasi-221005, U.P., INDIA



(Prof. Vikash Kumar Dubey)

Co-supervisor

Professor

School of Biochemical Engineering

Indian Institute of Technology

(Banaras Hindu University)

Varanasi- 221005

डा० विकेश कुमार दूबे
Dr. Vikash Kumar Dubey
आचार्य
Professor
जैव रासायनिक अभियांत्रिकी स्कूल
School of Biochemical Engin
भारतीय प्रौद्योगिकी संस्थान
Indian Institute of Techno
(का०हि०वि०) वाराणसी-2210
(B. H. U.) Varanasi-2210



(Prof. Vikash Kumar Dubey)

Coordinator

Professor

School of Biochemical Engineering

Indian Institute of Technology

(Banaras Hindu University)

Varanasi - 221005

समन्वयक
Coordinator
जैव रासायनिक अभियांत्रिकी स्कूल
School of Biochemical Engg
भारतीय प्रौद्योगिकी संस्थान
Indian Institute of Technology
(का०हि०वि०) वाराणसी-221005
(B. H. U.) Varanasi-221005

COPYRIGHT TRANSFER CERTIFICATE

Title of the Thesis: “**Natural and Synthetic based Polymeric Nanoparticles for Drug Delivery**”

Name of the Student: Rahul Kumar

Copyright Transfer

The undersigned hereby assigns to the Indian Institute of Technology (Banaras Hindu University), Varanasi all rights under copyright that may exist in and for the above thesis submitted for the award of the Ph.D. degree.

Date: 30/05/2022

Place: Varanasi

Rahul Kumar
(Rahul Kumar)

Note: However, the author may reproduce or authorize others to reproduce material extracted verbatim from the thesis or derivative of the thesis for author's personal use provided that the source and the Institute's copyright notice are indicated.

**DEDICATED TO MY LOVING
PARENTS AND SISTER
FOR THEIR LOVE, SUPPORT AND
ENCOURAGEMENT**

ACKNOWLEDGEMENTS

*First and foremost, I would like to express my sincere gratitude to my PhD supervisor **Dr. Pranjal Chandra** for his motivation, right direction, and kind support throughout. His continuous guidance helped me in my research and completion of the thesis. I could not have imagined having a better advisor and mentor for my PhD. work.*

*I would also like to thank my co-supervisor **Prof. Vikash Kumar Dubey** for his valuable help and support in my PhD. Work*

*I am thankful to RPEC members: **Dr. Sanjay Kumar**, School of Biochemical Engineering, IIT (BHU) and **Dr. Sanjeev Kumar Mahto**, School of Biomedical Engineering, IIT (BHU) for their fruitful suggestions.*

*I have been highly blessed with a friendly and cheerful group of fellow research scholars. I would like to express my heartfelt gratitude to my friends especially **Dr. Nitesh Singh Malan**, **Ms. Neelima Varshney**, **Mr. Deepak Khare**, **Dr. Vinod Kumar**, **Dr. Nupur Singh** for standing by my side.*

*Thanks to my lab colleagues **Supratim Mahapatra**, **Divya**, **Daphika S Dkhar**, and **Rohini Kumari** for their unconditional help and support.*

*I would like to express my gratitude towards the **CIF- IIT BHU** Varanasi for providing me instrumentation facilities.*

*I take this occasion to acknowledge the financial assistance provided by the **Ministry of Human Resource and Development** in the form of Teaching Assistantship.*

*I also wish to express thanks to **Prof. Mira Debnath (Das)** and **Late Dr. Ashish Kumar Singh** for their support during start of my PhD. tenure.*

*Finally, I bow my head humbly before the almighty **God** without whose consent and blessings, this work would have been impossible.*

Date: 30.06.2022



Place: IIT (BHU), Varanasi

(Rahul Kumar)

TABLE OF CONTENTS

List of Figure.....	XI
List of Tables.....	XVIII
List of abbreviations and symbols.....	XIX
Preface.....	XXI
Chapter I.....	1
1. General introduction.....	2
2. Types of NLBCs.....	6
2.1 Liposomes.....	6
2.2 Niosome.....	8
2.3 Solid lipid nanoparticles (SLNs).....	9
2.4 Nanostructured lipid carriers (NLCs).....	13
2.5 Lipid polymer hybrid nanoparticles (LPHNs).....	14
3. Preparation methods of NLBCs.....	16
3.1 Double emulsion method.....	16
3.2 Solvent injection method.....	18
3.3 Micro emulsion method	18
3.4 Ultra sonication method.....	19
3.5 Spray-drying method.....	19
3.6 Emulsification solvent evaporation method.....	19
3.7 Supercritical fluid method.....	20
3.8 Hot homogenization method.....	20
3.9 Cold homogenization method.....	21
4. Stability and Drawbacks.....	22
5. Lyophilization (Freeze-drying).....	24
6. Targeting moieties.....	27
6.1 Transferrin receptor.....	30
6.2 Folate receptor.....	33
6.3 Hyaluronic acid.....	35
6.4 Aptamer.....	37
6.5 Peptide.....	41

6.6	Growth factor as a target.....	45
6.7	Galactose.....	47
7.	Challenges in the scale-up of lipid-nanomedicines manufacturing: from.....	49
	laboratories to industry	
8.	Objective and goal of the study.....	51
9.	References.....	52
	Chapter II.....	65
1.	Introduction.....	66
2.	Material and methods.....	68
2.1	Materials.....	68
2.2.	Fabrication of Q laden NLBCs.....	69
2.3	Preparatin of N-acetyl-D-glucosylated Q-loaded NLBCs.....	70
2.4	<i>In vitro</i> fluorescence study using lectin-NADG nano bioconjugate.....	71
2.5	Encapsulation efficiency and percentage of drug loading.....	72
2.6	Scanning Elecron microscopy(SEM) of nano-bioconjgate.....	72
2.7	Analysis of particle diameter & charge distribution.....	73
2.8	Infrared spectroscopy (IR) characteization of nano-bioconjugate.....	73
2.9	X-ray characterization (XRD) of nano-bioconjugate.....	73
2.10	<i>In vitro</i> drug release study of nanobioconjugate.....	74
2.11	Cell culture and assessment of <i>in vitro</i> cell toxicity.....	74
2.12	Testing of statistical significance.....	75
2.13	Flow cytometry analysis.....	75
3.	Results and Discussions.....	76
3.1	Fluorescence studies.....	76
3.2	Encapsulation of drug content and drug loading.....	77
3.3	Morphological characterization of nano-bioconjugate.....	78
3.4	Average particle diameter and charge distribution measurement.....	79
3.5	IR characterization of nano bio-conjugate.....	81
3.6	X-ray characterization of nano-bioconjugate.....	82
3.7	Drug release kinetic.....	83
3.8	MTT assay.....	85
3.9	Analysis of cell apoptosis.....	86
4.	Conclusion.....	88

5. References.....	90
Chapter III.....	93
1.Introduction.....	94
2. Materials and methods.....	96
2.1 Preparation Q loaded LNs.....	96
2.2 Surface modification of Q-LNs with maleimide.....	97
2.3 Preparation of BSA conjugated with modified Q-LNs.....	97
2.4 Scanning electron microscope (SEM) studies.....	98
2.5 Particle size, size distribution, the surface charge of bioconjugate.....	98
2.6 Drug encapsulation efficiency.....	99
2.7 Fourier transformed infrared spectroscopy.....	100
2.8 X-ray diffraction study.....	100
2.9 <i>In vitro</i> release kinetic study.....	101
2.10 Cell culture.....	101
2.11 MTT assay.....	101
2.12 Confocal microscopy.....	102
2.13 DAPI staining.....	102
2.14 Propidium iodide staining.....	102
3. Results and Discussion.....	103
3.1 SEM analysis.....	103
3.2 Size measurement analysis/ Encapsulation efficiency.....	104
3.3 Fourier transformed infrared spectroscopy analysis.....	105
3.4 XRD analysis.....	106
3.5 Analysis of in vitro drug release kinetic.....	107
3.6 Cell viability study.....	108
3.7 Morphological analysis of MCF-7.....	110
4.Conclusion.....	111
5.References.....	112
Chapter IV.....	116
1. Introduction.....	117
2. Methods and Materials.....	119
2.1 Materials.....	119
2.2 Fabrication of LPBNPs.....	120
2.3 Lactoferrin conjugation with MTX-LPBNPs.....	120
2.4 Particle size analysis and assessment of surface charge.....	121
2.5 Drug encapsulation efficiency (DEE).....	122

2.6	Scanning electron microscopy (SEM).....	122
2.7	Powder X-ray diffractometry (XRD).....	123
2.8	Fourier transformed infrared spectroscopy.....	123
2.9	Methotrexate release profile.....	123
2.10	Storage stability.....	124
2.11	Cell culture and assessment of <i>in vitro</i> cellular toxicity.....	124
2.12	Fluorescence microscopy.....	125
3.	Result and Discussion	126
3.1	Particle size, size distribution, surface of hybrid nano-bio-conjugate.....	126
3.2	Analysis of morphological surface.....	129
3.3	Powder X-ray characterization of hybrid-nano-bioconjugate.....	131
3.4	Infrared spectroscopy analysis of hybrid-nano-bioconjugate.....	132
3.5	<i>In vitro</i> drug dissociation kinetics.....	133
3.6	Storage stability performance.....	135
3.7	Study of cell toxicity.....	136
3.8	Morphological analysis of MCF-7 cells induced with LPBNPs MTX-LPBNPs/MTX-LLPBNPs.....	140
4.	Conclusion.....	144
5.	References	145
	Chapter V.....	149
	Summary and Future Work.....	149

Figure No.	Figure description	Page No.
Figure 1.1	A pictorial representation of theranostics system including diagnosis/therapeutic agent along with nanocarrier.	4
Figure 1.2	Bar-graph showing number of research papers published each year from 2010 to 2022 in the online database "Scopus", searched using the keyword 'lipid nanocarriers and cancer theranostics'.	5
Figure 1.3	Timeline of liposome/Lipid based nanomedicine advancement. The discovery of liposomes; Enzyme entrapment into liposomes; Immunoliposomes; Procedures for liposome formation; pH-sensitive liposomes; Cationic lipids synthesized; Stealth liposomes; Transferrin receptor targeting; Temperature-sensitive liposomes; Cubosomes. The earliest approved lipid-based nanomedicine, Doxil; The earliest FDA-approved lipid - based nucleic acid (siRNA) drug Onpattro; First LNP-based mRNA vaccines for COVID-19 approved.	8
Figure 1.4	Schematic representation of five classes of lipid based nanocarriers (A) Liposomes (B) Niosomes (C) Solid lipid nanoparticles (D) Nano structured lipid carriers (E) Lipid polymer hybrid nanoparticles (LPHNs).	16
Figure 1.5	Schematic illustration of various techniques of synthesis of nano-lipid based carrier (A) Double emulsion method (B) Solvent injection method (C) Microemulsion method (D) Ultrasonication method.	17
Figure 1.6	Schematic illustration of various techniques for synthesis of nano lipid-based carriers (A) Spray drying method (B) Emulsification- solvent evaporation method (C) Supercritical fluid method (D) Hot/Cold homogenization method.	22
Figure 1.7	(A) The lipid bilayer exists in two phases. The lipid head group surrounds the water channel before drying (Hexagonal phase). The lipid bilayer is packed into a two-dimensional lattice after	27

drying (Ribbon phase). (B) Orientation of lipid bilayer before and after drying in the presence and absence of sugars.

- Figure 1.8** Schematic representation of ligand conjugated nanocarriers. 32
(A) Synthesis of Tf conjugated nanocarriers and its interactions with cognate molecule. (B) The FA conjugated drug-loaded micelle and liposome and their internalization in tumor-bearing mice. (C) EDC-mediated crosslinking of HA on the surface of lipid nanocarriers. (D) RNA based aptamer and aptamer decorated nanocarrier and its interaction with the cognate receptor.
- Figure 1.9** Schematic illustration of ligand conjugated nanocarriers. 41
(A) NGR-conjugated thermosensitive liposome containing CPPs-DOX for detection of receptor and enhancing the DOX biodistribution. (B) Schematic representation of the synthesis of Fab' conjugated nanoparticle. Initially, reduction of anti-EGFR Fab'2 to Fab' fragment through Tris/2-carboxyethyl phosphine hydrochloride (TCEP) and generating three active thiol groups (-SH), which further react with maleimide group expressed on the nanoparticle surface. (C) EGF expressed nanocarrier for cancer theranostics of curcumin and doxorubicin in A-431 tumor cells. (D) Step by step synthesis of galactosylated conjugated drug loaded SLNs. Initially ring opening of galactose molecule and further cross-linked with amino group of stearyl amine exposed on the surface of SLNs through the EDC/NHS bioconjugate chemistry.
- Figure 2.1** Schematic representation of the synthesis of N-acetyl D- 68
glucosylated Q-loaded nano lipid-based carrier and its cellular internalization through receptor-mediated endocytosis.
- Figure 2.2** Chemical reactions for N-acetyl D-glucosamine with Poly-l 70
lysine.
- Figure 2.3** Fluorescence spectroscopy emission spectra of the lectin-NADG 77
complex. (a) Emission spectra of lectin reduced on gradual

addition of NADG. The red curve elucidates the concentration of lectin whereas the blue curve indicates a decrease in fluorescence intensity of lectin on the reaction between 5×10^{-8} and 6×10^{-7} M of NADG. (b) Logarithmic plot of the lectin-NADG system at room temperature.

- Figure 2.4** Scanning electron microscopy (SEM) photograph of the nano-bio material (a) Q-NLBCs and (b) NADG-Q-NLBCs. 79
- Figure 2.5** Distribution of hydrodynamic diameter in (nm) for (a) Q-NLBCs and (b) NADG-Q-NLBCs. 80
- Figure 2.6** The infrared spectrum of Q-NLBCs and NADG-Q-NLBCs in the region of $4000-400 \text{ cm}^{-1}$. 82
- Figure 2.7** X-ray diffractogram of (a) NLBCs and (b) NADG-Q-NLBCs between $2\theta = 2^\circ$ to $2\theta = 90^\circ$ at a scanning speed of $0.03^\circ/\text{second}$. 83
- Figure 2.8** Drug release kinetics of Q from NADG-Q-NLBCs (*in vitro*) in phosphate buffer saline for (a) Zero-order and (b) First-order at physiological pH with a significance level ($p \leq 0.05^*$). 84
- Figure 2.9** Cell toxicity studies on MCF-7 cells (*in vitro*). The histograms represent the % cell viability against NLBCs, free Q, and NADG-Q-NLBCs for five different concentrations at the cell's density of 4×10^5 cells/well. Values are reported as (mean \pm standard error) and significance level as ($***p < 0.001$, $**p < 0.01$ and $*p < 0.05$). All experiments were performed in triplicates. 86
- Figure 2.10** Flow cytometry images of MCF-7 cells (a) Cells treated with NLBCs for 48 h and dot quadrant Q3 showing the viable cells and Q1 represents the necrotic cells (b) Cells treated with Q-NLBCs for 48 h, quadrants Q4 and Q2 showing the early and late apoptotic cells, respectively and Q1 represents the necrotic cells (c) Cells treated with NADG-Q-NLBCs for 48 h, quadrants Q4 and Q2 indicating the early and late apoptotic cells, 88

respectively and Q1 represents the necrotic cells. All experiments were performed in triplicates.

Figure 3.1	Schematic representation of the synthesis of BSA conjugated Q loaded lipid nanocarriers (LNs) and its cellular internalization through receptor mediated endocytosis.	98
Figure 3.2	Chemical reactions for maleimide functionalization and BSA conjugation.	100
Figure 3.3	SEM image of (a) void LNs (b) Q-loaded LNs (c) BSA conjugated Q-LNs.	103
Figure 3.4	FT-IR spectra in the section of 4000–400 cm^{-1} (a) void LNs(b) Q-loaded LNs (c) BSA conjugated Q-LNs.	106
Figure 3.5	X-ray diffraction image of (a) void LNs and (b) BSA-Q-loaded LNs.	107
Figure 3.6	Release kinetic studies of BSA-Q-LNs (a) Zero-order release kinetics (b) First order release kinetic.	108
Figure 3.7	The cytotoxic effect of free Q, Q-loaded LNs, and BSA conjugated Q-LNs at various concentrations of Q on MCF-7.	110
Figure 3.8	The confocal image of MCF-7, Row 1 cells treated with void LNs, Q-LNs, and BSA-Q-LNs; PI staining. Row 2 cells treated with void LNs, Q-LNs, and BSA-Q-LNs; DAPI staining.	111
Figure 4.1	Schematic illustration of the synthesis of lactoferrin conjugated MTX-LPBNPs using one-step precipitation technique and its cellular internalization through receptor-mediated endocytosis.	121
Figure 4.2	Distribution of hydrodynamic diameter in (nm) (A) MTX-LPBNPs and (B) MTX-LLPBNPs.	129
Figure 4.3	Scanning electron microscopy (SEM) photograph (A-B), and EDX images of the hybrid NPs (C-D). (A) SEM showing the MTX-LPBNPs (B) SEM showing the MTX-LLPBNPs. (C)EDX chemical mapping (inlet) and elemental composition for elements presence in MTX-LPBNPs (D) EDX chemical	130

mapping (inlet) and elemental composition for elements presence in MTX-LLPBNPs.

- Figure 4.4** X-ray diffractograms of the hybrid system, scanning over $2\theta = 10^\circ$ to $2\theta = 80^\circ$ at a scanning speed of $0.03^\circ/\text{second}$ using Cu K α radiation ($\lambda=1.54\text{\AA}$) (A) LPBNPs and (B) MTX-LLPBNPs. 131
- Figure 4.5** The infrared spectrum of MTX-LPBNPs (Red curve) and MTX-LLPBNPs (Blue curve); was scanned on a scale of 4000 cm^{-1} to 800 cm^{-1} with a resolution of 4 cm^{-1} . 133
- Figure 4.6** The MTX release profile of constructed hybrid nanobioconjugate (LLPBNPs) was performed for 200 h. Dialysis was performed against phosphate buffer saline (pH 7.4) at room temperature using a dialysis bag. UV spectrophotometer was used to quantify the amounts of MTX concentration. Data are reported as (mean \pm standard error) and significance level as ($p\leq 0.05^*$) (A) zero-order kinetics and (B) first-order kinetics. 136
- Figure 4.7** Cell toxicity studies of LPBNPs, MTX, MTX-LPBNPs, and MTX-LLPBNPs on MCF-7 for 24.0 h of incubation. Treatment was studied in the five groups. In the first, second, third, fourth, and fifth groups, the MTX concentration was taken 2.0, 4.0, 6.0, 8.0, and 10.0 $\mu\text{g/mL}$, respectively. In the MTX-LPBNPs and MTX-LLPBNPs formulation, a similar concentration of MTX was taken in each group. However, the LPBNPs were taken as a control in the groups. Values are reported as (mean \pm standard error) and significance level as ($***p < 0.001$, $**p < 0.01$ and $*p < 0.05$). 139
- Figure 4.8** Cell toxicity studies of LPBNPs, MTX, MTX-LPBNPs, and MTX-LLPBNPs on MCF-7 for 48.0 h of incubation. Treatment was studied in the five groups. In the first, second, third, fourth, and fifth groups, the MTX concentration was taken 2.0, 4.0, 6.0, 8.0, and 10.0 $\mu\text{g/mL}$, respectively. In the MTX-LPBNPs and MTX-LLPBNPs formulation, a similar concentration of MTX was taken in each group. However, the LPBNPs were taken as a 140

control in the groups. Values are reported as (mean \pm standard error) and significance level as (** $p < 0.001$, ** $p < 0.01$ and * $p < 0.005$).

Figure 4.9 Fluorescence microscopy photographs of the MCF-7 after 24.0 h of treatment with LPBNPs, MTX-LPBNPs, and MTX-LLPBNPs at equivalent MTX, 10.0 ($\mu\text{g/mL}$). The fluorescence signals from the cells were illustrated in **Row 1-3** after 24.0 h of incubation. (**Row 1-A**) DAPI staining, blue signals show the nucleus induced with LPBNPs. (**Row 1-B**) rhodamine-conjugated phalloidin staining, red signals show the cytoskeleton induced with LPBNPs. (**Row 1-C**) merged distribution of DAPI & rhodamine-conjugated phalloidin. (**Row 2-A**) DAPI staining, blue signals show the nucleus induced with MTX-LPBNPs. (**Row 2-B**) rhodamine-conjugated phalloidin staining, red signals show the cytoskeleton induced with MTX-LPBNPs. (**Row 2-C**) merged distribution of DAPI & rhodamine-conjugated phalloidin. (**Row 3-A**) DAPI staining, blue signals show the nucleus induced with LLPBNPs. (**Row 3-B**) rhodamine-conjugated phalloidin staining, red signals show cytoskeleton induced with MTX-LLPBNPs. (**Row 3-C**) merged distribution of DAPI & rhodamine-conjugated phalloidin. The scale bar is 50 μm for fluorescence images. 142

Figure 4.10 Fluorescence microscopy photographs of the MCF-7 after 48.0 h of treatment with LPBNPs, MTX-LPBNPs, and MTX-LLPBNPs at equivalent MTX, 10.0 ($\mu\text{g/mL}$). The fluorescence signals from the cells were illustrated in **Row 1-3** after 48.0 h of incubation. (**Row 1-A**) DAPI staining, blue signals show the nucleus induced with LPBNPs. (**Row 1-B**) rhodamine-conjugated phalloidin staining, red signals show the cytoskeleton induced with LPBNPs. (**Row 1-C**) merged distribution of DAPI & rhodamine-conjugated phalloidin. (**Row 2-A**) DAPI staining, blue signals show the nucleus induced with MTX-LPBNPs. (**Row 2-B**) rhodamine-conjugated phalloidin 143

staining, red signals show the cytoskeleton induced with MTX-LPBNPs. (**Row 2-C**) merged distribution of DAPI & rhodamine-conjugated phalloidin. (**Row 3-A**) DAPI staining, blue signals show the nucleus induced with LLPBNPs. (**Row 3-B**) rhodamine-conjugated phalloidin staining, red signals show cytoskeleton induced with MTX-LLPBNPs. (**Row 3-C**) merged distribution of DAPI & rhodamine-conjugated phalloidin. The scale bar is 50 μm for fluorescence images

Table No.	Table description	Page No.
Table 1.1	List of various types of lipid-based nanocarriers.	11
Table 1.2	List of ligands and their target molecules with nanocarriers.	28
Table 2.1	Determination of amount of Q in the designed nanobioconjugate.	78
Table 3.1	Particle size distribution and encapsulation efficiency.	105
Table 4.1	Particle size, size distribution, zeta potential, and drug encapsulation efficiency of MTX-LPBNPs and MTX-LLPBNPs and data represent mean \pm SD, n=3.	127
Table 4.2	Storage stability performance of optimized MTX-LLPBNPs	135

List of abbreviations and symbols

PEG-PE	Polyethylene glycol-phosphatidyl ethanolamine
DPPC	Dipalmitoyl phosphatidylcholine
DOPE	Dioleoyl phosphatidyl ethanolamine
DOPC	1,2-dioleoyl-sn-glycero-3-phosphocholine
DSPE	1,2-distearoyl-sn-glycero-3-phosphoethanolamine
PEG	polyethylene glycol
HSPC	L- α -phosphatidylcholine hydrogenated (Soy)
DOTA	1,4,7,10- Tetraazacyclododecane-1,4,7,10-tetraacetic acid
DEPC	1,2-Dierucoyl-snglycero-3-phosphocholine
DSPC	1,2-distearoyl-sn-glycero-3-phosphocholine
DPPE	dipalmitoyl-phosphatidylethanolamine
EPOPC	1-palmitoyl-2-oleoyl-sn-glycero-3-ethylphosphocholine
FITC	Fluorescein isothiocyanate
EDC	ethyl-3-(3-dimethylamine propyl carbodiimide
NHS	N-hydroxy succinimide
DOTAP	1,2-Dioleoyl-3-trimethylammonium propane
QDs	Quantum dots
MSPC	Monostearoyl phosphatidylcholine
CHS-ED-LA	5-cholesten-3 β -yl) 4-oxo-4-[2-(lactobionyl amido) ethylamido] butanoate
	Eyeblink

NADG	N-acetyl-d-glucosamine
NLBCs	Nano-lipid-based carriers
Q	Quercetin
XRD	X-ray diffractometry
SEM	Scanning electron microscopy
FT-IR	Fourier transformed infrared spectroscopy
DLS	Direct light scattering
MTT	3-(4,5-Dimethylthiazol-2-Yl)-2,5-Diphenyltetrazolium Bromide
BSA	Bovine serum albumin
LN _s	Lipid nanocarriers
DMAP	4-(dimethyl amino) pyridine
LLPBNPs	Lactoferrin conjugated lipid polymer-based nanoparticles
LPBNPs	Lipid polymeric based nanoparticles
MTX	Methotrexate
PCL	Polycaprolactone

PREFACE

In view of drug delivery, diverse delivery vehicles including natural and synthetic polymeric nanoparticles have been greatly investigated till date. In general, micelles, dendrimers, cellulose, gelatin, lipid, chitosan, alginate, poly (D, L-lactide), poly (D, L-glycoside), poly(lactide-co-glycoside), and poly-caprolactone have been employed as drug delivery vehicles. However, we are interested to select lipid-based nanoparticle/nanocarrier for targeted anticancer drug delivery. Cancer is one of the major health-related issues affecting the population worldwide and subsequently accounts for the second-largest death. Genetic and epigenetic modifications in oncogenes or tumor suppressor genes affect the regulatory systems that lead to the initiation and progression of cancer. Therefore, in view of cancer burden worldwide, we have targeted the cancer cells for drug delivery. Conventional methods, including chemotherapy/radiotherapy/appropriate combinational therapy and surgery, are being widely used for theranostics of cancer patients. Surgery is useful in treating localized tumors, but it is ineffective in treating metastatic tumors, which spread to other organs and result in a high recurrence rate and death. Also, the therapeutic application of free drugs is related to substantial issues such as poor absorption, solubility, bioavailability, high degradation rate, short shelf-life, and low therapeutic index. Therefore, these limitations can be sorted out using NLBCs as promising drug delivery carriers. Still, at most, they fail to achieve site targeted drug delivery and detection. This can be achieved by using the concept of theranostics which is a combination of diagnostic and therapeutic agents. Selecting a specific ligand/antibody as a diagnostic tool is being highly utilized since its cognate receptor molecule is expressed on the surface of the cancer cell.

We have designed the study in four different sections, where in the first part; we have developed N-acetyl-D-glucosamine (NADG) coupled quercetin-loaded (Q) nano-lipid-based carriers (NADG-Q-NLBCs) where NADG has been covalently conjugated on the surface of NLBCs containing quercetin as anti-cancer drugs. The constructed nano-bioconjugate was

characterized by various techniques, and the *in vitro* drug release profiles were examined using zero and first-order kinetic models. The characterization data confirmed the morphology, size, charge distribution, crystallinity, and chemical interactions among the various moieties of the nano-bioconjugate. Further, the synthesized NADG-Q-NLBCs were applied to target the human breast cancer cells (MCF-7), which interestingly showed a more cytotoxic effect compared to the lone NLBCs and free Quercetin. The flow cytometry study confirmed that NADG-Q-NLBCs induced apoptosis in MCF-7 cells in a targeted manner. The percentage of early apoptotic cells was found to be 25% in the case of NADG-Q-NLBCs, which is almost 2.5 times higher than the Q-NLBCs. However, the number of viable cells reached the maximum when treated with NLBCs. The present investigation suggests that the constructed nano-bioconjugate could be a capable carrier of drugs with sustained pharmacokinetics and improved physicochemical properties.

In the next section, we have attempted to conjugate BSA to maleimide functionalized lipid surface for cancer theranostics. The BSA was conjugated with C1 carbon of maleimide through a thiol reaction. The BSA conjugated quercetin-loaded lipid nanocarriers (BSA-Q-LNs) were spherical in structure with a shell size of 296.43 ± 4.90 nm. The encapsulation efficiency of BSA-Q-LNs was found to be $76 \pm 0.3\%$. Further, BSA conjugation on carrier surface was confirmed from the shift in FT-IR, XRD peak. The release kinetic of Q- loaded LNs formulation was best fitted in a first-order kinetic model suggesting an early burst of Q followed by sustain rate of release. The Q-loaded LNs and BSA-Q-LNs displayed improved cytotoxicity in the human breast cancer cell line (MCF-7) as compared to free Q.

Further, we have designed and developed a new system that further improves the stability, and crystallinity, and releases the kinetic profile of the free drugs. In this system, lipid and polycaprolactone (PCL) were blended and then lactoferrin as a diagnostic agent has been conjugated on the surface of the hybrid system using covalent bonding. A lactoferrin-conjugated lipid polymer-based nanoparticles (LLPBNPs) encapsulating methotrexate (MTX)

as a potential anticancer drug candidate was constructed via a facile one-step precipitation method. The designed hybrid-nano-bioconjugate exploits both the characteristic features of natural lipids and the biocompatible polymer. The physiochemical properties of the constructed hybrid-nano-bioconjugate were thoroughly characterized by Infrared Spectroscopy, Scanning Electron Microscopy, EDX, Dynamic Light Scattering, and X-ray Diffraction techniques. The general sizes of the particles are obtained in the range of 520-650 nm with a polydispersity of 0.140-0.163 that does not possess a broad size distribution. Further, the encapsulation efficiency of the MTX in LLPBNPs systems was assessed, which was found to be 84.0 ± 1.5 %. The *in vitro* drug release kinetics were analytically examined using the zero and first-order kinetic models. These models revealed that the drug dissociation initially shows the first-order model followed by a sustained rate of drug delivery. The morphological changes of the nucleus and F-actin cytoskeleton of the cancer cells were studied using molecular binding probes DAPI and rhodamine-conjugated phalloidin, respectively.

Thus, this work is a concept-based comparative investigation of N-acetyl-d-glucosamine decorated nano-lipid-based carriers, BSA conjugated quercetin-loaded lipid nanocarriers, and lactoferrin conjugated lipid-polymer nano-bio-hybrid for cancer theranostics. In the future, the constructed system may overcome the problem of multiple drug resistance.